arXiv:hep-ex/9608009v1 14 Aug 1996

TAUP 2349-96
July 1996

The transition from the photoproduction to the DIS region *

Aharon Levy

School of Physics and Astronomy

Raymond and Beverly Sackler Faculty of Exact Sciences

Tel–Aviv University, Tel–Aviv, Israel

Abstract

This is a review of the existing ideas in modelling the transition from the photoproduction ($Q^2 = 0$) to the deep inelastic scattering region. The available data of the proton structure function are analyzed from the point of view of the total $\gamma^* p$ cross section behavior with W and the results are compared to different parameterizations. The question whether DIS processes are hard or soft is discussed.

*Talk presented at the DIS 96 Workshop, Rome, 15-19 April, 1996.

1 Introduction

One of the aims of building HERA was to study the deep inelastic scattering (DIS) region with data at low x and high Q^2. Yet, recently efforts are being made to get to lower and lower Q^2 values in the low x region in order to study the transition from photoproduction to the DIS regime. The main motivation for looking at the transition region is the following: at $Q^2 = 0$ the dominant processes are of non–perturbative nature and are well described by the Regge picture. As Q^2 increases, the exchanged photon is expected to shrink and one expects perturbative QCD to take over. What can one learn from the transition between soft processes (low virtuality) and hard processes (high virtuality)? Where does the change take place? Is it a sudden transition or a smooth one? The transition should shed light on the interplay between soft and hard interactions. In addition, being able to describe this region has a practical necessity: it is needed for calculating radiative corrections.

The purpose of this talk is to review the ideas in modelling the low x and low Q^2 region [1].

2 The models

2.1 Donnachie and Landshoff (DL)

Donnachie and Landshoff [2] found a simple Regge picture describing all hadron–hadron cross sections with a sum of two terms, that of a pomeron exchange and that of a reggeon. They showed this picture to describe also real photoproduction cross sections. They extended the picture for virtual photons ($\gamma^*, Q^2 < 10$ GeV^2) to see what is the expected contribution of the non–perturbative mechanism to higher Q^2 [3]. The main interest is in the low x region where the pomeron dominates and thus the question of interest is what is the contribution of the 'soft' pomeron at intermediate Q^2.

2.2 Capella, Kaidalov, Merino, Tran–Than–Van (CKMT)

In this picture [4] there is no 'soft' or 'hard' pomeron, there is just one 'bare' pomeron. At low Q^2 absorptive corrections (rescattering) give a pomeron with an effective intercept of $1 + \Delta_0 (\Delta_0 \sim 0.08)$. If one uses an eikonal approach, the bare intercept becomes $1 + \Delta_1 (\Delta_1 \sim 0.13)$. A more complete absorptive calculation results in $1 + \Delta_2 (\Delta_2 \sim 0.24)$. The absorptive corrections decrease rapidly with Q^2. They parametrize the data with this behavior of the pomeron up to $Q^2 < 5$ GeV^2 and use it then as initial conditions to a pQCD evolution.

2.3 Badelek and Kwiecinski (BK)

Badelek and Kwiecinski [5] describe the low Q^2 region by using the generalized vector dominance model (GVDM): the proton structure function F_2 is represented by the contribution of a large

number of vector mesons which couple to virtual photons. The low mass ones, ρ, ω, ϕ contribute mainly at low Q^2, while the higher mass are determined by the asymptotic structure function F_2^{AS} which is described by pQCD. The total structure function is given by a Q^2 weighted sum of the two components.

2.4 Abramowicz, Levin, Levy, Maor (ALLM)

This parameterization [6] is based on a Regge motivated approach extended into the large Q^2 regime in a way compatible with QCD expectations. This approach allows to parametrize the whole x, Q^2 phase space, fitting all the existing data.

2.5 Some general comments

The DL parametrization provides a good way to check to what value of Q^2 can the simple 'soft' pomeron picture be extended. It is not meant to be a parameterization which describes the whole DIS regime. The CKMT and BK parametrizations are attempts to get the best possible presentation of the initial conditions to a pQCD evolution. The ALLM does not use the regular pQCD evolution equation but parametrizes the whole of the DIS phase space by a combination of Regge and QCD motivated parametrizations.

All parameterizations make sure that as $Q^2 \to 0$ also $F_2 \to 0$ linearly with Q^2.

3 Details of the parametrizations

3.1 The DL parameterization

The proton structure function F_2 is given by

$$F_2(x, Q^2) \sim A\xi^{-0.0808}\phi(Q^2) + B\xi^{0.4525}\psi(Q^2), \tag{1}$$

where ξ is the rescaled variable

$$\xi = x\left(1 + \frac{\mu^2}{Q^2}\right), \tag{2}$$

with x being the Bjorken–x and the scale variable μ has different values for different flavors: for u and d quarks $\mu = 0.53$ GeV, for the strange quark s, $\mu = 1.3$ GeV and for the charm quark c, $\mu = 2$ GeV. The two functions $\phi(Q^2)$ and $\psi(Q^2)$ make sure that the structure function vanishes linearly with Q^2 as $Q^2 \to 0$,

$$\phi(Q^2) = \frac{Q^2}{Q^2 + a} \qquad \psi(Q^2) = \frac{Q^2}{Q^2 + b}. \tag{3}$$

The four parameters A, B, a and b are constrained so as to reproduce the total real photoproduction data,

$$\frac{A}{a}(\mu^2)^{-0.0808} = 0.604 \qquad \frac{B}{b}(\mu^2)^{0.4525} = 1.15. \tag{4}$$

In addition there is also a higher–twist term $ht(x, Q^2)$ contributing to the structure function,

$$ht(x, Q^2) = D\frac{x^2(1-\xi)^2}{1+\frac{Q^2}{Q_0^2}}, \tag{5}$$

with the parameters $D = 15.88$ and $Q_0 = 550$ MeV.

3.2 The CKMT parameterization

Contrary to the DL parameterization, the CKMT assumes that the power behavior of x is Q^2 dependent,

$$F_2(x, Q^2) = Ax^{-\Delta(Q^2)}(1-x)^{n(Q^2)+4}\left(\frac{Q^2}{Q^2+a}\right)^{1+\Delta(Q^2)} + Bx^{1-\alpha_R}(1-x)^{n(Q^2)}\left(\frac{Q^2}{Q^2+b}\right)^{\alpha_R}, \tag{6}$$

where α_R is the Reggeon trajectory intercept, the power $n(Q^2)$ is given by

$$n(Q^2) = \frac{3}{2}\left(1+\frac{Q^2}{Q^2+c}\right) \tag{7}$$

and the power behavior of x is given by

$$\Delta(Q^2) = \Delta_0\left(1+\frac{Q^2}{Q^2+d}\right). \tag{8}$$

The constant parameters are determined by the requirement that F_2 and the derivative $\frac{dF_2}{d\ln Q^2}$ at $Q^2 = Q_0^2$ to coincide with that obtained from the pQCD evolution equations. They can do so at $Q_0^2 = 2$ GeV^2, provided a higher–twist term is added to that of pQCD,

$$F_2(x, Q^2) = F_2^{pQCD}(x, Q^2)\left(1+\frac{f(x)}{Q^2}\right) \tag{9}$$

for $Q^2 \geq Q_0^2$. The values of the parameters are: $A = 0.1502$, $a = 0.2631$ GeV^2, $\Delta_0 = 0.07684$, $d = 1.117$ GeV^2, $b = 0.6452$ GeV^2, $\alpha_R = 0.415$, $c = 3.5489$ GeV^2.

3.3 The BK parameterization

The proton structure function is written as the sum of two terms, a vector meson part (V) and a partonic part (par),

$$F_2(x, Q^2) = F_2^V(x, Q^2) + F_2^{par}(x, Q^2). \tag{10}$$

The part representing the contribution from vector mesons which couple to the virtual photon is given by

$$F_2^V(x,Q^2) = \frac{Q^2}{4\pi}\Sigma_V \frac{M_V^4 \sigma_V(W^2)}{\gamma_V^2 (Q^2+M_V^2)^2}, \tag{11}$$

where $\gamma_V^2/(4\pi)$ is the direct photon vector meson coupling, W is the $\gamma^* p$ center of mass energy and σ_V is the total Vp cross section. The sum is over all vector meson satisfying $M_V^2 < Q_0^2$, where M_V is the mass of the vector meson and Q_0 is a parameter.

The partonic part of the structure function is given by the expression

$$F_2^{par}(x,Q^2) = \frac{Q^2}{Q^2+Q_0^2} F_2^{AS}(\bar{x}, Q^2+Q_0^2), \tag{12}$$

where the asymptotic structure function F_2^{AS} is given by pQCD at the scaled value of

$$\bar{x} = \frac{Q^2+Q_0^2}{W^2+Q^2-M^2+Q_0^2}, \tag{13}$$

where M is the proton mass. In practice the parameterization uses $Q_0^2 = 1.2$ GeV^2 and thus sums over the contribution of the 3 lightest vector mesons ρ, ω and ϕ.

3.4 The ALLM parameterization

This parameterization attempts to cover the whole of x, Q^2 region above the resonances ($W^2 > 3$ GeV^2), at the expense of introducing more parameters than the other parameterizations. The proton structure function has the form

$$F_2(x,Q^2) = \frac{Q^2}{Q^2+M_0^2}\left(F_2^{\mathcal{P}}(x,Q^2) + F_2^{\mathcal{R}}(x,Q^2)\right), \tag{14}$$

where M_0 is the effective photon mass. The functions $F_2^{\mathcal{P}}$ and $F_2^{\mathcal{R}}$ are the contribution of the pomeron $\mathcal{P}$ or Reggeon $\mathcal{R}$ exchanges to the structure function. They take the form

$$\begin{aligned} F_2^{\mathcal{P}}(x,Q^2) &= c_{\mathcal{P}}(t) x_{\mathcal{P}}^{a_{\mathcal{P}}(t)} (1-x)^{b_{\mathcal{P}}(t)}, \\ F_2^{\mathcal{R}}(x,Q^2) &= c_{\mathcal{R}}(t) x_{\mathcal{R}}^{a_{\mathcal{R}}(t)} (1-x)^{b_{\mathcal{R}}(t)}. \end{aligned} \tag{15}$$

The slowly varying function t is defined as

$$t = \ln\left(\frac{\ln\frac{Q^2+Q_0^2}{\Lambda^2}}{\ln\frac{Q_0^2}{\Lambda^2}}\right). \tag{16}$$

The two scaled variables $x_{\mathcal{P}}$ and $x_{\mathcal{R}}$ are modified Bjorken–x variables which include mass parameters $M_{\mathcal{P}}$ and $M_{\mathcal{R}}$ which can be interpreted as effective pomeron and reggeon masses:

$$\begin{aligned} \frac{1}{x_{\mathcal{P}}} &= 1 + \frac{W^2-M^2}{Q^2+M_{\mathcal{P}}^2}, \\ \frac{1}{x_{\mathcal{R}}} &= 1 + \frac{W^2-M^2}{Q^2+M_{\mathcal{R}}^2}. \end{aligned} \tag{17}$$

4 Comparison to data

The proton structure function has been measured [7] in a wide range of x and Q^2. A constructive way to display them [8] over a wide kinematical range is to use the relation between F_2 and the total $\gamma^* p$ cross section,

$$\sigma^{\gamma^* p}(W^2, Q^2) = \frac{4\pi^2\alpha}{Q^2} \frac{1}{1-x} \left(1 + \frac{4M^2x^2}{Q^2}\right) F_2(x, Q^2). \tag{18}$$

In this expression the Hand definition of the flux of virtual photons is used.

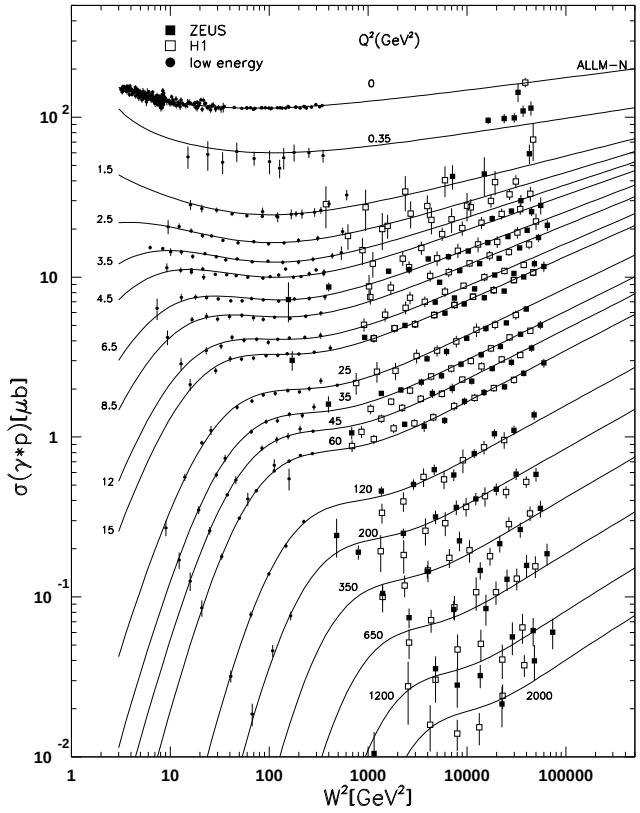

Figure 1: The total $\gamma^* p$ cross section as function of W^2 from the F_2 measurements for different Q^2 values. The lines are the expectations of the ALLM parameterization.

Figure 1 presents the dependence of $\sigma_{tot}^{\gamma^* p}$, obtained through equation 18 from the measured F_2 values [9, 10], on the square of the center of mass energy, W^2, for fixed values of the photon virtuality Q^2. The new preliminary very low Q^2 measurements of the ZEUS collaboration [11], as well as those of the NMC collaboration presented at this workshop [12] are included in the figure. Also shown are the measurements of the total real photoproduction cross sections. While the data below Q^2=1 GeV^2 shows a very mild W dependence, which resembles that of the real photon data, the trend changes as Q^2 increases. Note that for higher values of Q^2 one sees the typical threshold behavior for the case when $W^2 < Q^2$ [13]. The curves are the results of a new ALLM type parameterization which includes now also the data from E665 [14], those from NMC [15] and the published HERA [16] data.

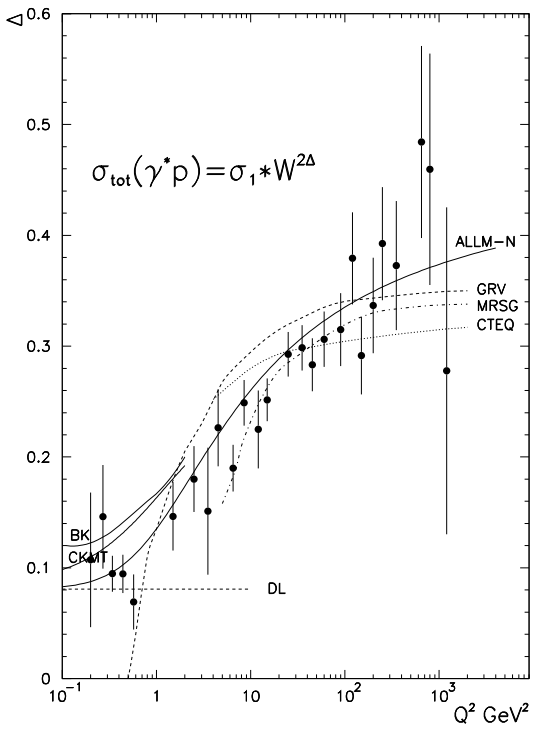

Figure 2: The Q^2 dependence of the parameter Δ obtained from a fit of the expression $\sigma_{tot}^{\gamma^* p} = \sigma_1 W^{2\Delta}$ to the data in each Q^2 bin. The curves are the expectations of the parameterizations mentioned in the text.

Instead of comparing the data as presented in figure 1 with the different parameterizations, it is more economical as well as instructive to study the energy dependence of the $\gamma^* p$ cross section for fixed Q^2 values [17]. In order to see how the slope of the W dependence changes with Q^2, the cross section values in the region where $W^2 \gg Q^2$ were fitted to the form $\sigma_{tot}^{\gamma^* p} = \sigma_1 W^{2\Delta}$ for each fixed Q^2 interval. The resulting values of Δ from the fit are plotted against Q^2 in figure 2. Similar results have been obtain by the H1 collaboration [10] who use only their own data to fit the structure function measurements to the form $F_2 \sim x^{-\Delta}$. Also included in the figure are the recent preliminary results of the ZEUS collaboration [11] in the region $0.2 < Q^2 < 0.8$ GeV^2. One can see the slow increase of Δ with Q^2 from the value of 0.08 at Q^2=0, to around 0.2 for $Q^2 \sim$ 10–20 GeV^2 followed by a further increase to around 0.3–0.4 at high Q^2. One would clearly profit from more precise data, expected to come soon.

The curves are the expectations of the DL, BK, CKMT, and the updated ALLM parameterization, which includes also some of the recent HERA data in its fit. In addition, the expectations of the GRV [18], CTEQ [19] and MRSG [20] are also shown.

The DL parameterization can describe the data up to $Q^2 \sim 1$ GeV^2. All the others give in general the right features of the Q^2 behavior with a smooth transition from soft to hard interactions with an interplay between the two in the intermediate Q^2 range.

5 DIS processes - hard or soft?

What have we learned from the behavior of the data with Q^2? What are we actually measuring? At low Q^2 the photon is known to have structure. Does F_2 still measure the structure of the proton? Bjorken [21] pointed out that physics is not frame dependent. The structure of the proton alone has no meaning. One has to study the $\gamma^* p$ interaction.

Let us look at the structure of a photon. It is a well known fact that real photon behave like hadrons when interacting with other hadrons. One way to understand this is by using the argument of Ioffe [22]: the photon can fluctuate into a $q\bar{q}$ pair. The fluctuation time is given by

$$t_f = \frac{2E_\gamma}{m^2_{q\bar{q}}} \tag{19}$$

where E_γ is the photon energy in the rest system of the proton and $m_{q\bar{q}}$ is the mass of the $q\bar{q}$ system into which the photon fluctuates. The Vector Dominance Model assumes that the fluctuation of the photon is into vector mesons, $m_{q\bar{q}} \simeq m_V$, where m_V is the vector mesom mass. As long as $t_f \gg t_i$, where the interaction time $t_i \approx r_p$, with r_p being the proton radius, the photon interacts as if it were a hadron. When the photon becomes virtual with a negative square mass of Q^2, its fluctuation time becomes

$$t_f = \frac{2E_\gamma}{m^2_{q\bar{q}} + Q^2} \tag{20}$$

and thus at low energies and moderate Bjorken x, the fluctuation time becomes small and the virtual photon behaves like a point–like structureless object, consistent with the DIS picture described above.

However, at high energies or equivalently in the low x region studied at HERA, the fluctuation time of a virtual photon can be expressed as

$$t_f \approx \frac{1}{2Mx} \tag{21}$$

where M is the proton mass. This can be derived easily from formula (20), assuming $m^2_{q\bar{q}} \approx Q^2$ [23]. Thus in the HERA regime, a photon of virtuality as high as $Q^2 \sim 2 - 3 \times 10^3$ GeV^2 can fluctuate into a $q\bar{q}$ pair, which will survive till arrival on the proton target.

The photon can fluctuate into typically two configurations. A large size configuration will consist of an asymmetric $q\bar{q}$ pair with each quark carrying a small transverse momentum k_T (fig. 3(a)). For a small size configuration the pair is symmetric, each quark having a large k_T (fig. 3(b)). One expects the asymmetric large configuration to produce 'soft' physics, while the symmetric one would yield the 'hard' interactions.

In the aligned jet model (AJM) [24] the first configuration dominates while the second one is the 'sterile combination' because of color screening. In the photoproduction case ($Q^2 = 0$), the small k_T configuration dominates. Thus one has large color forces which produce the hadronic component, the vector mesons, which finally lead to hadronic non–perturbative final states of

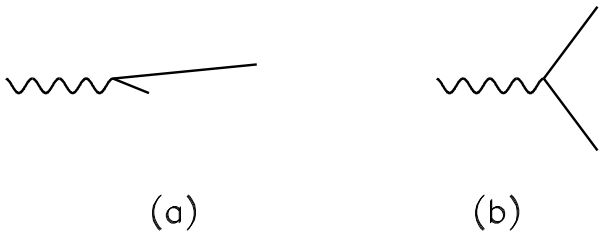

Figure 3: Fluctuation of the photon into a $q\bar{q}$ pair in (a) asymmetric small k_T configuration, (b) into a symmetric large k_T configuration

'soft' nature. The symmetric configuration contributes very little. In those cases where the photon does fluctuate into a high k_T pair, color transparency suppresses their contribution.

In the DIS regime ($Q^2 \neq 0$), the symmetric contribution becomes bigger. Each such pair still contributes very little because of color transparency, but the phase space for the symmetric configuration increases. However the asymmetric pair still contribute also to the DIS processes. In fact, in the quark parton model (QPM) the fast quark becomes the current jet and the slow quark interacts with the proton remnant resulting in processes which look in the $\gamma^* p$ frame just like the 'soft' processes discussed in the $Q^2 = 0$ case. So there clearly is an interplay between soft and hard interactions also in the DIS region.

This now brings up another question. We are used by now to talk about the 'resolved' and the 'direct' photon interactions. However, if the photon always fluctuates into a $q\bar{q}$ pair even at quite large values of Q^2, what does one mean by a 'direct' photon interaction? To illustrate the problem, let us look at the diagram describing the photon–gluon fusion, which is usually considered in leading order a direct photon interaction and is shown in figure 4(a). An example of a resolved process is shown in figure 4(b) where a photon fluctuates into a $q\bar{q}$ pair with a given k_T, following by the interaction of one of the quarks with a gluon from the proton to produce a quark and a gluon with a given p_T.

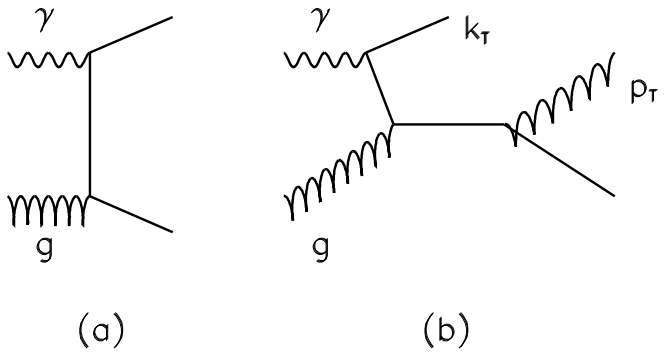

Figure 4: Diagrams describing examples of (a) 'direct' photon process, (b) 'resolved' photon process

In the diagram shown in figure 4(b) there are two scales, k_T and p_T. The classification of the process as 'direct' or 'resolved' depends on the relations between the two scales. If $k_T \ll p_T$

we call it a resolved photon interaction, while in the case of $k_T \gg p_T$ one would consider this as a direct photon interaction. Practically in the latter case the p_T is too small to resolve the gluon and the quark jets as two separate jets, thus making it look like the diagram in figure 4(a). At low Q^2 the more likely case is that of $k_T \ll p_T$ and thus the resolved photon is the dominant component, while at high Q^2 the other case is more likely. A yet open question is how does one deal with the case where $k_T \sim p_T$.

6 Summary

The energy behavior of the $\gamma^* p$ cross section shows that there is a smooth transition between the Q^2 region where there is a mild energy dependence to that where the energy behavior is steeper. It happens somewhere in the region of about 1 GeV^2. Does this tell us where soft interactions turn into hard ones? In order to understand the structure of the dynamics, one has to isolate in the transition region the specific configurations in k_T and p_T for a better insight of what is happening.

Acknowledgments

It is a pleasure to thank Halina Abramowicz and Lonya Frankfurt for giving me some better insight of the interplay between soft and hard interactions. Special thanks to Giullio d'Agostini and his committee for organizing such an excellent workshop.

References

[1] For a recent review see B.Badelek, J.Kwiecinski, Rev. Mod. Phys, to be published (1996).

[2] A. Donnachie, P.V. Landshoff, *Phys. Lett.* **B296** (1992) 227.

[3] A. Donnachie, P.V. Landshoff, *Nucl. Phys.* **B244** (1984) 322; A. Donnachie, P.V. Landshoff, *Phys. Lett.* **C61** (1994) 139.

[4] A.B. Kaidalov et al., *Sov. J. Nucl. Phys.* **44** (1986) 468; A. Capella et al., *Phys. Lett.* **B337** (1994) 358.

[5] J. Kwiecinski, B. Badelek, *Zeit. Phys.* **C43** (1989) 251; B. Badelek, J. Kwiecinski, *Phys. Lett.* **B295** (1992) 263.

[6] H. Abramowicz et al., *Phys. Lett.* **B269** (1991) 465; A. Marcus, *Energy dependence of the $\gamma^* p$ cross section*, M.Sc. Thesis, Tel–Aviv University (1996).

[7] For a recent review see F. Eisele Invited talk at International Europhysics Conference on High Energy Physics (HEP 95), Brussels, Belgium, 27 Jul - 2 Aug 1995, DESY 95–229 (1995).

[8] A.Levy, DESY 95–003 (1995).

[9] ZEUS Coll., M. Derrick et al., *Zeit. Phys.* **C69** (1996) 607.

[10] H1 Coll., S. Aid et al., DESY 96–039 (1996).

[11] Q.Zhu for the ZEUS collaboration, this workshop.

[12] E.Rondio for the NMC collaboration, this workshop.

[13] A.Levy, U.Maor, *Phys. Lett.* **B182** (1986) 108.

[14] E665 Coll., Preliminary results presented by A.V.Kotwal in *The XXXth Recontres de Moriond, QCD and High Energy Interactions*, March 1995.

[15] NMC Coll., M.Arneodo et al., CERN–PPE–95–138 (1995).

[16] ZEUS Coll., M.Derrick et al., *Zeit. Phys.* **C65** (1995) 379; H1 Coll., T.Ahmed et al., *Nucl. Phys.* **B439** (1995) 471.

[17] A.Levy, Invited talk at International Europhysics Conference on High Energy Physics (HEP 95), Brussels, Belgium, 27 Jul - 2 Aug 1995, DESY 95–209 (1995).

[18] M. Gluck, E. Reya, A. Vogt, *Zeit. Phys.* **C67** (1995) 433.

[19] R. Brock et al., *Rev. Mod. Phys.* **67** (1995) 157.

[20] A.D. Martin, W.J. Stirling, R.G. Roberts, *Phys. Lett.* **B354** (1995) 155.

[21] J.D Bjorken, Proceedings of the International Workshop on DIS and related subjects, Eilat, 1994, p. 151.

[22] B.L. Ioffe, *Phys. Lett.* **30** (1969) 123.

[23] H. Abramowicz, L. Frankfurt, M. Strikman, DESY 95–045 (1995).

[24] J.D. Bjorken, Proceedings of the International Symposium on Electron and Photon interactions at High Energies, Cornell, 1971, p. 281.